

A BAYESIAN SPATIAL MIXTURE MODEL FOR FMRI ANALYSIS

Maya Geliazkova

ABSTRACT. We develop, implement and study a new Bayesian spatial mixture model (BSMM). The proposed BSMM allows for spatial structure in the binary activation indicators through a latent thresholded Gaussian Markov random field. We develop a Gibbs (MCMC) sampler to perform posterior inference on the model parameters, which then allows us to assess the posterior probabilities of activation for each voxel. One purpose of this article is to compare the HJ model and the BSMM in terms of receiver operating characteristics (ROC) curves. Also we consider the accuracy of the spatial mixture model and the BSMM for estimation of the size of the activation region in terms of bias, variance and mean squared error. We perform a simulation study to examine the aforementioned characteristics under a variety of configurations of spatial mixture model and BSMM both as the size of the region changes and as the magnitude of activation changes.

1. Introduction. Many fMRI experiments have a common objective of identifying active voxels in a neuroimaging data set. This is done in single subject

ACM Computing Classification System (1998): I.5.1.

Key words: spatial mixture models, CAR model, ROC analysis, procedure, bias, variance, mean squared error.

experiments for example by performing individual voxel-wise tests of the null hypothesis that the observed time course is not significantly related to an assigned reference function [1, 5]. A voxel activation map is then constructed by applying a thresholding rule to the resulting t-statistics. Typically, the task-related activation is expected to occur in clusters rather than in isolated single voxels. Mixture models were proposed for the independent activation case by Everitt and Bullmore [6], and were extended by Hartvig and Jensen [9] to account for spatial clustering of activation. Two Bayesian spatial mixture models have been proposed in the literature. Woolrich et al. [19] propose a spatial mixture model with three groups representing nonactivation, activation and deactivation. The authors approximate the discrete activation class labels with a vector of continuous weights w , meant to approximate the delta function $I(A_i = k)$, where i is the corresponding voxel and k is the activation group index. Spatial clustering is accounted for by using a conditional autoregressive model on a logistic transformation of the weight vector. However, it is unclear how well this approximation to the discrete labels likelihood works.

Smith et al. apply an Ising model [10, 11, 18] to generate spatial structure in the prior distributions. This results in a fast single-site sampler for generating the posterior distributions. However, the Ising prior may have some potential drawbacks such as not being adaptive to the degree of voxel activation.

In this paper we develop, implement and study a new Bayesian spatial mixture model (BSMM). The proposed BSMM allows for spatial structure in the binary activation indicators through a latent thresholded Gaussian Markov random field, somewhat analogous to a spatial probit model. We develop a Gibbs (MCMC) sampler to perform posterior inference on the model parameters, which then allows us to assess the posterior probabilities of activation for each voxel. This model also accounts appropriately for the variability in the model parameters, unlike the spatial mixture model of Hartvig and Jensen [9], which was based solely on maximum pseudo-likelihood estimates. A purpose of this article is to compare the HJ model and the BSMM in terms of receiver operating characteristics (ROC) curves. Another purpose of this paper is to consider the accuracy of the spatial mixture model and the BSMM for estimation of the size of the activation region in terms of bias, variance and mean squared error (MSE). We perform a simulation study to examine the bias, variance, and MSE of a variety of configurations of spatial mixture model and BSMM both as the size of the region changes and as the magnitude of activation changes.

2. Spatial Mixture Models. In the following we assume that the investigator has already performed an analysis to obtain a statistical parametric

map, which is a matrix of test statistics corresponding to the null hypothesis of no task-related activation. These could come for example from a series of univariate regression analysis at each voxel, where the independent variables include a linear drift term and a variable reflecting the task such as hemodynamic response function or “boxcar” predictor. Under the null hypothesis, these test statistics typically have a t_ν distribution, where ν is large, so that it can be approximated by a normal distribution.

In 1999, Everitt and Bullmore [6] proposed an alternative approach for detecting activated voxels in the human brain under a cognitive task. They fitted a finite mixture distribution to the observed distribution of the test statistic. The mixture distribution has two components, one of which accounts for the activated voxels and the other represents the non-activated voxels. They also estimated the proportion of voxels which are activated, denoted by p , and the parameter that characterizes the activation distribution μ using maximum likelihood methods. Posterior probabilities of activation are expressed for each voxel in terms of these estimated parameters. These posterior probabilities can be thresholded (e.g., taking 0.5 as a threshold) to identify which voxels are activated and which are not. I would like to point out that the approach is not fully Bayesian. There are only point estimates of the model parameters. The authors used only the point estimates in order to compute the posterior probabilities of activation, rather than posterior distribution of the model parameters.

Hartvig and Jensen [9] extended this mixture model to allow for association between neighboring voxels in terms of activation status. This association mimics the clustering of activation typically seen in fMRI data.

Let A_i be the indicator for voxel i being activated. In terms of A_i , the nonspatial mixture distribution model is given by

$$f(t_i; \mu, p) = (1 - p)f(t_i|A_i = 0) + pf(t_i|A_i = 1; \mu),$$

where p represents the marginal probability of a voxel (e.g., voxel i) being activated, $P(A_i = 1)$. Then the posterior probability of activation for voxel i assuming independent voxels is

$$P(A_i = 1|t_i) = \frac{\hat{p}f(t_i|A_i = 1; \hat{\mu})}{f(t_i; \hat{\mu}, \hat{p})}.$$

Hartvig and Jensen [9], however, consider not only voxel i , but also neighbors, in determining activation at voxel i . They denote by C the set of $k+1$ voxels, given voxel i together with its k neighbors. A_C is the vector of activation in C , denoted $A_C = (A, A_1, \dots, A_k)$, and t_C is the vector of the test statistic for activation in

C , denoted $t_C = (t, t_1, \dots, t_k)$. The posterior probabilities of activation have the form

$$\begin{aligned} P(A = 1|t_C) &= \sum_{A_C:A=1} P(A_C|t_C) \\ &= \sum_{A_C:A=1} \frac{f(t_C|A_C)P(A_C)}{P(t_C)} \\ &\propto \sum_{A_1=0}^1 \dots \sum_{A_k=0}^1 f(t_C|A_C = (1, A_1, \dots, A_k))P(A_C = (1, A_1, \dots, A_k)). \end{aligned}$$

Under conditional independence of t_i given A_i , the density of t_C given A_C can be written as

$$f(t_C|A_C = a_C) = f(t|a) \prod_{j=1}^k f(t_j|a_j),$$

where $f(t|a)$ is the density of t given $A = a$. Hartvig and Jensen [9] present three models for the joint prior distribution for A_C , denoted $P(A_C)$. We will describe two of them; the third one is omitted for brevity.

2.1. Model 1. For an activation configuration a_C let l be the number of ones (or active voxels) in a_C , $l = a + a_1 + \dots + a_k$.

Model 1 defines the marginal probability of activation in neighborhood C as

$$P(A_C = a_C) = \begin{cases} q_0 & \text{if } l = 0 \\ q_1 & \text{if } 0 < l \leq k+1 \end{cases}$$

The model may be parameterized through the mixture probability p of a voxel being activated as $p = q_1 2^k$ or $q_1 = p 2^{-k}$ and $q_0 = 1 - (2 - 2^{-k})p$. The conditional probabilities of activation given the values of t_i in the neighborhood are calculated as

$$P(A = 1|t_C) = \left\{ 1 + \frac{f(t|0)}{f(t|1)} \left[1 + \left(\frac{q_0}{q_1} - 1 \right) r \right] \right\}^{-1},$$

where

$$r = \left(\prod_{j=1}^k \left(1 + \frac{f(t_j|1)}{f(t_j|0)} \right) \right)^{-1}.$$

2.2. Model 2. Model 2 defines the marginal probability of activation in a neighborhood to be related to the number of active voxels in the neighborhood,

$$P(A_C = a_C) = \begin{cases} q_0 & \text{if } l = 0 \\ \phi\gamma^{l-1} & \text{if } 0 < l \leq k + 1 \end{cases}$$

The model can be parameterized through the marginal probability p of a voxel being activated. A simple combinatorial argument gives that $p = \phi(1 + \gamma)^k$. The parameter γ can be interpreted as a measure of correlation of neighboring voxels. The last parameter q_0 is given by the constraint that the probabilities must sum up to 1. Hartvig and Jensen [9] show that the conditional probability of activation given the values t_i in the neighborhood is given by

$$P(A = 1|t_C) = \left\{ 1 + \frac{f(t|0)}{f(t|1)} \left[\gamma^{-1} + \frac{1 - \phi(1 + \gamma)^{k+1}/\gamma}{\phi} \tilde{r}(\gamma) \right] \right\}^{-1},$$

where

$$\tilde{r}(\gamma) = \left(\prod_{j=1}^k \left(1 + \gamma \frac{f(t_j|1)}{f(t_j|0)} \right) \right)^{-1}.$$

In order to estimate δ , p , and γ , Hartvig and Jensen [9] propose to maximize the pseudo-likelihood function

$$L = \sum_{i=1}^k \log f(t_{C_i}; \mu, p),$$

where $f(t_{C_i})$ is the density function of the neighborhood centered at voxel i .

Hartvig and Jensen [9] do not recommend Model 3. Geliazkova and Logan [7] study the performance of the various spatial mixture models and recommend Model 2 with eight neighbors.

2.3. Bayesian Spatial Mixture Model. Now we will describe the proposed Bayesian Spatial Mixture model. The parameters of the model are γ , β and μ . In this model γ is a latent Gaussian spatial process, β is the overall level of activation, and μ is the mean of the test statistics of the active voxels. We assume a mixture model for the z-statistics testing for a task-related activation at each voxel, depending on voxel i 's unknown binary activation status, denoted A_i . The density function of the normal distribution is $P(z_i) = \frac{1}{2\pi} \exp\left(-\frac{1}{2} \frac{(z_i - \mu)^2}{\sigma^2}\right)$, where μ is the mean and σ is the standard deviation. The active voxels follow

normal distribution with mean μ and standard deviation 1 $N(\mu, 1)$, while the nonactive voxels follow normal distribution with mean 0 and standard deviation 1 $N(0, 1)$.

Assuming conditional independence given A_i , the likelihood is

$$L = \prod_i \left[\frac{1}{2\pi} \exp\left(-\frac{1}{2}z_i^2\right) \right]^{1-A_i} \left[\frac{1}{2\pi} \exp\left(-\frac{1}{2}(z_i - \mu)^2\right) \right]^{A_i},$$

where μ is the mean of the test statistics of the active voxels.

The spatial model for the binary activation indicators is induced by a latent Gaussian spatial process $\gamma = (\gamma_1, \dots, \gamma_m)$, where $A_i = I(\beta + \gamma_i > 0)$ and I is an indicator function. Here β reflects the overall level of activation in the image. The process γ is assumed to follow a Gaussian conditional autoregressive (CAR) model [2].

The conditional specification of the CAR model will be given on the next several lines, where the symbol \sim means follow.

$$P(\gamma_i | \gamma_{-i}, \phi) \sim N\left(\bar{\gamma}_i, \tilde{\phi}_i^{-1}\right),$$

where $\sum_{j \sim i} \frac{w_{ij}\gamma_j}{w_{i+}} = \bar{\gamma}_i$, the symbol \sim on that line means that voxel i is a neighbor of j , $\tilde{\phi}_i^{-1} = \frac{\phi}{w_{i+}}$. $\gamma_{-i} = \{\gamma_j, j \neq i\}$, $w_{ij} = 1$ if $i \sim j$ (i.e., voxel i is a neighbor of voxel j), otherwise $w_{ij} = 0$ and $w_{i+} = \sum_j w_{ij}$ is the number of neighbors of voxel i .

The joint density of γ in the CAR model has the form

$$P(\gamma_1, \dots, \gamma_m | \phi) \propto \exp\left(-\frac{1}{2\phi} \sum_{i \neq j} w_{ij}(\gamma_i - \gamma_j)^2\right),$$

where m is the total number of voxels in the image.

The hyperprior for β is assumed to come from a $N(\mu_\beta, \sigma_\beta^2)$ distribution, so that

$$P(\beta) \propto \exp\left(-\frac{(\beta - \mu_\beta)^2}{2\sigma_\beta^2}\right).$$

The hyperparameters μ_β and σ_β^2 on β , which regulates the proportion of active voxels, is selected so that *a priori* there is a low likelihood of a voxel being active.

To complete the Bayesian specification of the prior distributions, we consider a prior distribution for μ . We will take a normal prior for μ with mean μ_0 and standard deviation $\frac{\mu_0}{3}$.

$$P(\mu) \propto \exp\left(-\frac{(\mu - \mu_0)^2}{2 \cdot \frac{\mu_0^2}{9}}\right).$$

This standard deviation is chosen so that μ will be nonnegative with high probability.

Closed-form expressions for the full posteriors can be obtained using this specification, leading to a fast implementation of the Gibbs sampler. We are interested in using this model to estimate the posterior probability of activation of voxel i given the t-statistics map $p_i = P(A_i = 1|t_1, \dots, t_m) = E(A_i|t_1, \dots, t_m)$. Unfortunately this mean is intractable. Let $(A_1^{(l)}, \dots, A_m^{(l)}, \mu^{(l)}, \beta_0^{(l)})$ for $l = 1, \dots, L$ be a set of Gibbs samples from the joint posterior of $A_1, \dots, A_m, \mu, \beta_0$. Then considering voxel i for example, $A_i^{(1)}, \dots, A_i^{(L)}$ is a sample from the posterior marginal distribution of A_i given t_1, \dots, t_m . From this the posterior probability of activation for voxel i can be estimated by

$$P(A_i = 1|t_1, \dots, t_m) = \frac{A_i^{(1)} + \dots + A_i^{(L)}}{L}.$$

3. FMRI Simulation Study.

Part 1: ROC curves. The first part of the simulation study compares the characteristics of these spatial thresholding procedures in terms of their sensitivity to voxel activation. We use ROC curves [15] to display the results. ROC curves are a plot of the sensitivity (on the y-axis) versus 1 minus the specificity (on the x-axis), plotted over a range of test statistic thresholds. Each threshold determines an (x,y) point on the curve. Here sensitivity is the probability of identifying an active voxel as active because it is over the threshold, while 1 minus the specificity is the false positive rate, or the probability of incorrectly identifying an inactive voxel as active because it is above the threshold. ROC curves range from (0,0) to (1,1), and ideally the researcher wants the curve to be as close to the upper left point (1,0) as possible. ROC analysis has been used in several prior studies to validate approaches in fMRI [4, 13, 14, 17, 20].

In each case, data is generated to simulate a t-statistic SPM where the regions of activation (ROAs) are known. A 64 by 64 image slice is selected for

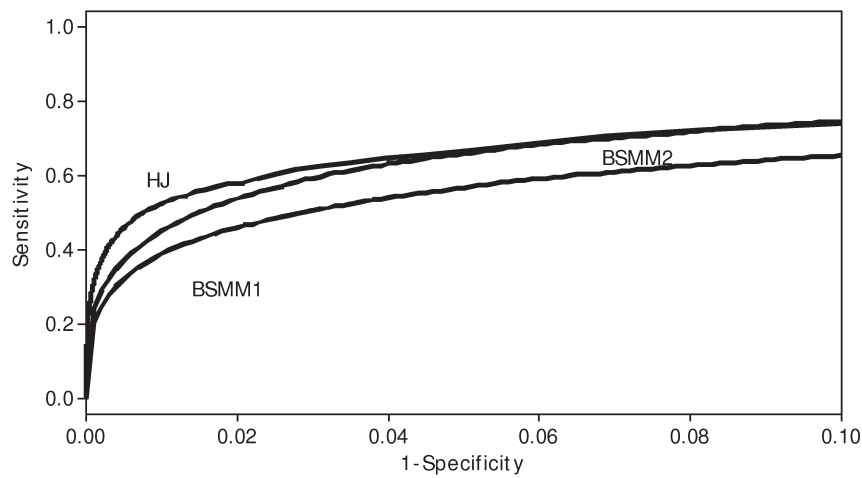


Fig. 1. ROC curve for 3 by 3 region

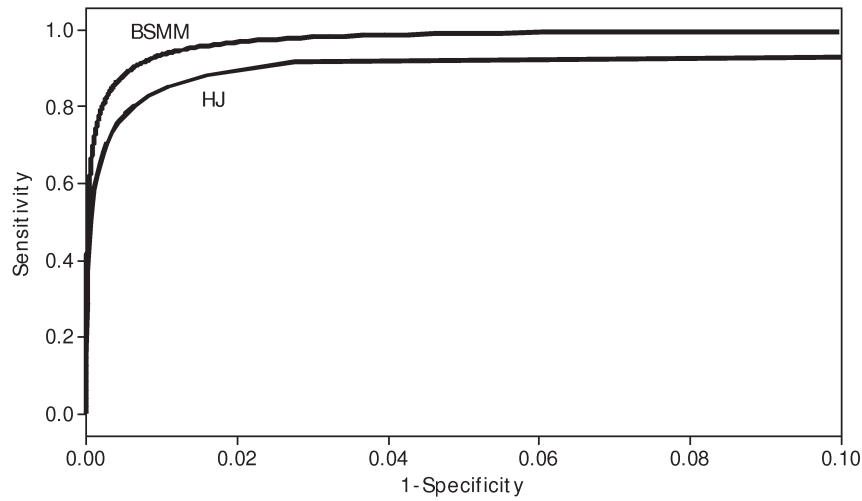


Fig. 2. ROC curve for 7 by 7 region, BSMM

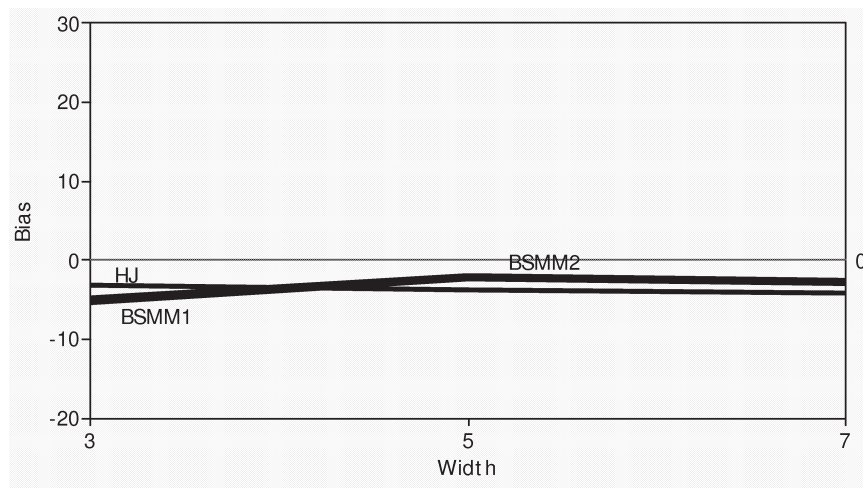


Fig. 3. Bias of ROA size estimate as a function of the width, BSMM

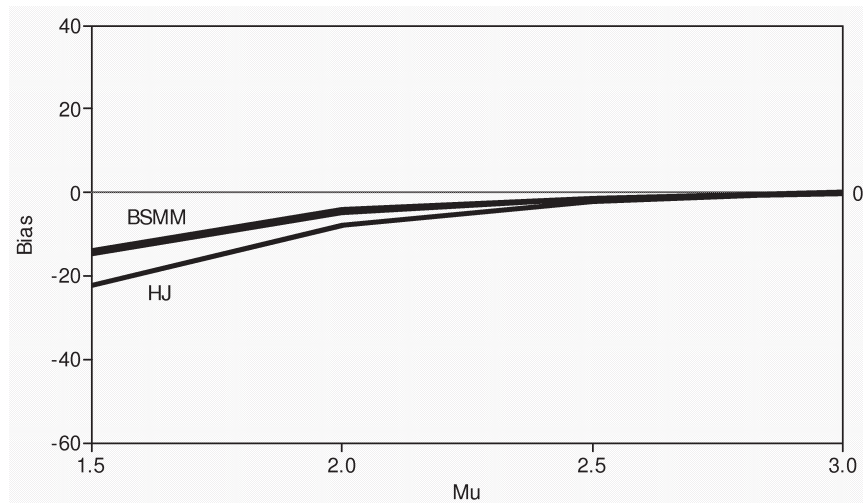


Fig. 4. Bias of ROA size estimate as a function of the mean of the activated voxels, μ , BSMM

analysis within which two square ROAs are designated to have activation. For this slice, simulated fMRI t-statistics (assuming large d.f.) outside the ROAs are generated from a $N(0,1)$ distribution, while inside the ROAs they are generated from a $N(\mu,1)$. Here μ can be interpreted as the mean of the standardized t-statistics for activated voxels. We use $\mu = 1.5$ and ROAs varying from 3 by 3 to 7 by 7. Figure 9 illustrates sample 7 by 7 ROAs as considered in the two parts of the simulation study. To estimate the (x,y) point on the ROC curve, first a fixed threshold in terms of the test statistic is set. Then using that threshold value, the sensitivity and $(1 - \text{Specificity})$ is computed for each image. These are then averaged across 500 simulated images to generate the (x,y) point. This is repeated for a range of thresholds to generate a curve. This is similar to the approach used in Logan et al. [12]. A total of 500 simulations for each scenario are used in all simulations. The spatial mixture model is done using a neighborhood of eight neighbors, and is thresholded over a range of posterior probability of activation.

Part 2: Estimation of the size of ROA. In this simulation study, we measure the bias and the variance of the estimate of the size of the activation region for each procedure. The size of the activation region is the number of truly active voxels across both ROAs, while the estimated size is the number of voxels which are declared active by one of the thresholding procedures. The true number of active voxels ranges from 18 for a 3 by 3 region to 98 for 7 by 7 regions. Two scenarios are considered; in the first we study the bias and variance of each procedure as the size of the activation regions gets larger, and in the second we compare the bias and variance as the magnitude of activation changes. The data generation model is as in Part 1. In the first scenario, we vary the dimensions of the square ROAs from 3 by 3 to 5 by 5 to 7 by 7, with $\mu = 2.25$. In the second scenario, we use two 7 by 7 square ROAs while varying μ from 1.5 to 3.0 by increments of 0.5. Spatial mixture model 2 is made using a neighborhood of eight neighbors, and is thresholded at a 0.5 posterior probability of activation.

4. A Real Data Example. A bilateral finger-tapping experiment was performed to illustrate the spatial thresholding procedures investigated earlier. To generate the functional data, bilateral finger tapping was performed in a block design with 8 epochs of 16 s off and 16 s on, followed by 20 s off. Scanning was performed using a GE 3T scanner, in which 15 axial slices of size 96×96 were acquired. A mask was applied so that only the interior 64×64 image is used. Each voxel has dimensions 2 mm cubic voxels with TE=48 ms. Observations were taken every TR = 2,000 ms so that there are 138 in each voxel. Data from a single axial slice through the motor cortex were selected for analysis. A

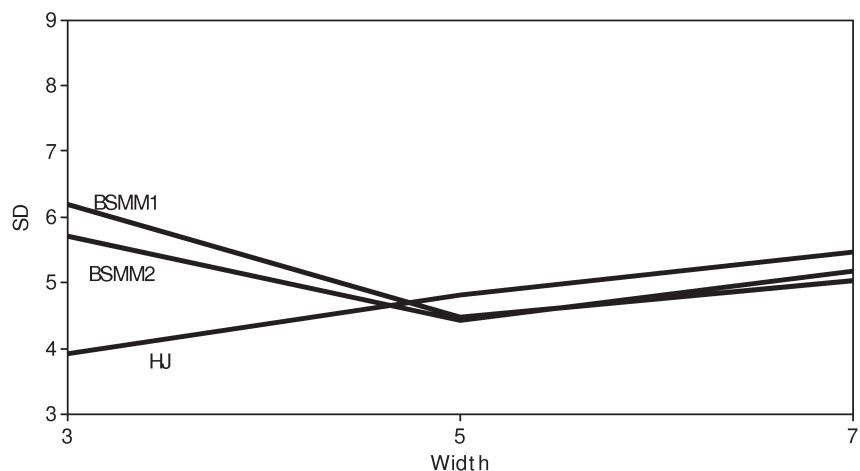


Fig. 5. SD of ROA size estimate as a function of the width, BSMM

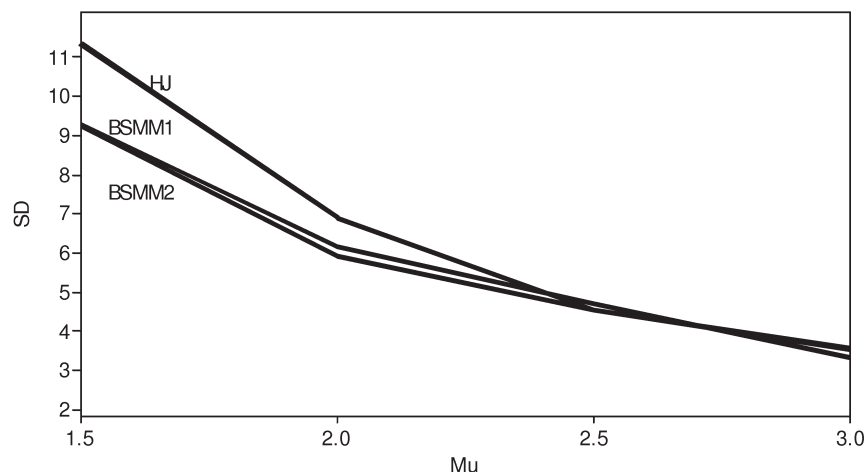


Fig. 6. SD of ROA size estimate as a function of the mean of the activated voxels, μ , BSMM

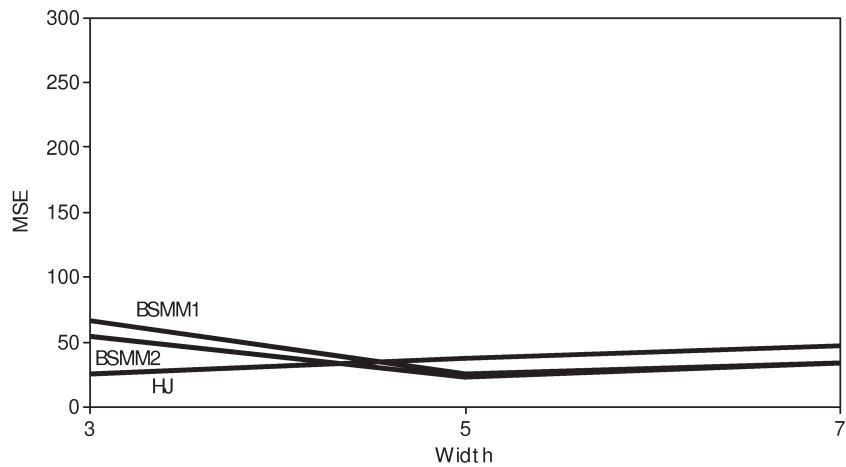


Fig. 7. MSE of ROA size estimate as a function of the width, BSMM

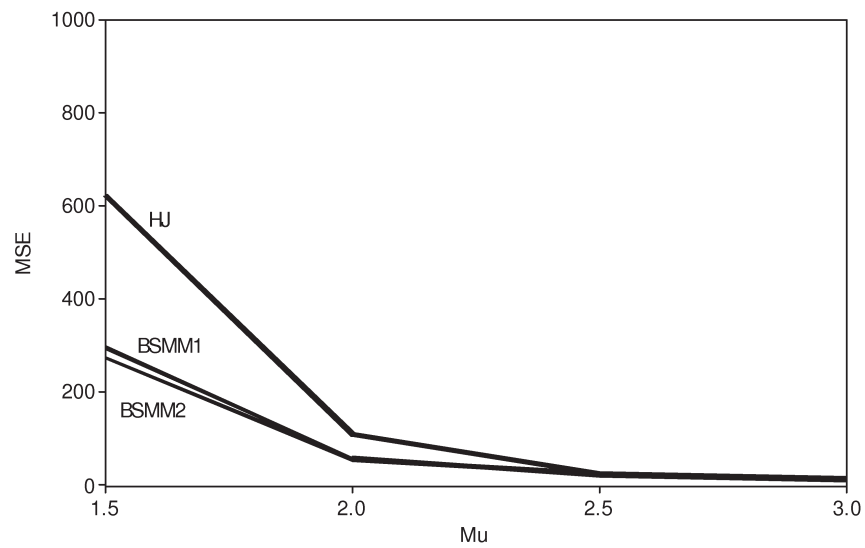


Fig. 8. MSE of ROA size estimate as a function of the mean of the activated voxels, μ , BSMM

multiple regression model was fit to the data with an intercept, a time trend and a reference function. The time trend was a column of counting numbers from a linear time trend. The first 6 seconds were omitted to remove warm-up effects, and the reference function was a “boxcar” shape, shifted by 6 s to match the hemodynamic response function. The “boxcar” predictor is simply a $[-1, 1]$ indicator of whether the subject is engaged in the cognitive task or not. Temporal AR(1) autocorrelation was checked, found to be minimal, and so was not adjusted for. Each of the methods discussed were applied to the dataset.

5. Results.

Simulation Study Part 1: ROC curves. The ROC curves for the Bayesian spatial mixture model are given in Figure 1 for 3 by 3 ROAs and in Figure 2 for 7 by 7 ROAs. As a comparison I also show the HJ spatial mixture model in the same figure. The BSMM with a prior on β_0 of $N(-1.5, 1)$ (BSMM2) for 3 by 3 activation regions seems to be performing almost as well as the HJ model. However the BSMM with a prior of $N(-3, 1)$ (BSMM1) seems to be less sensitive than the HJ model and BSMM2 models. For 7 by 7 activation regions the ROC curves for BSMM1 and BSMM2 turn out to be almost identical. This indicates that for a larger region of activation the results are not sensitive to the prior on β_0 . Also, the BSMM is more sensitive to activation than the HJ model.

Simulation Study Part 2. Estimation of Size of ROA. Figure 3 and Figure 4 contains the bias estimate of the size of the ROA for the BSMM and HJ procedure. The BSMM seems to outperform the HJ model slightly. Both models have a bias that approaches 0 as μ gets large.

Figure 5 and Figure 6 contain the SD estimation of the size of the ROA for the BSMM and HJ procedures. In Figure 5 the SD is plotted against the width of the square ROA, while in Figure 6 the SD is plotted against the magnitude of activation. The BSMM seems to outperform the HJ model slightly, although the difference diminish as μ gets large.

Figure 7 and Figure 8 contain the MSE of the estimates of the size of the ROA for the BSMM and HJ procedure. In Figure 7 the MSE is plotted against the width of the square ROA, while in Figure 8 the MSE is plotted against the magnitude of activation. As before, the BSMM seems to outperform the HJ model slightly, but the difference diminish as μ gets large.

Real Example. Figure 10 shows the results of the Hartvig and Jensen spatial mixture model, with posterior probabilities thresholded at 0.5. Figure 11 and Figure 12 show the results of the BSMM with a prior on β_0 $N(-3, 1)$

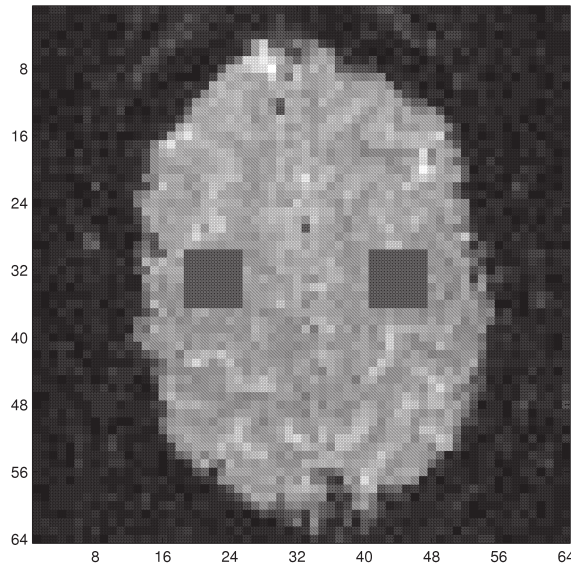


Fig. 9. 7 by 7 regions of activation

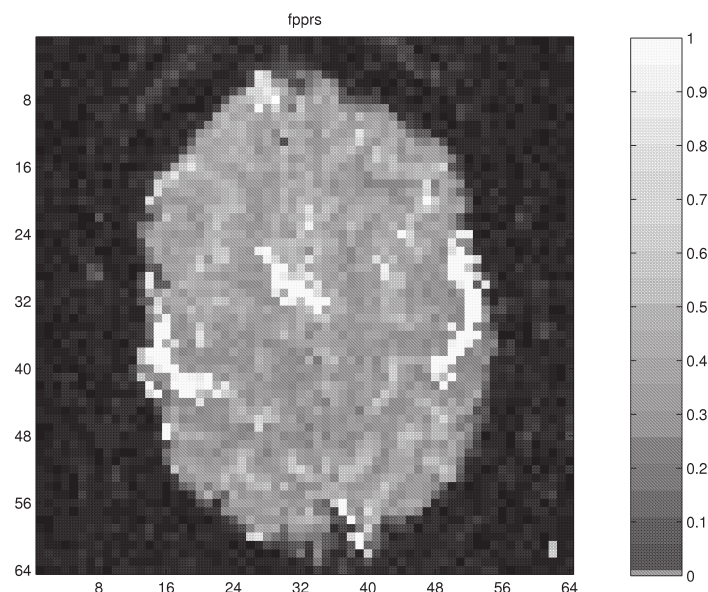


Fig. 10. Posterior probabilities from HJ

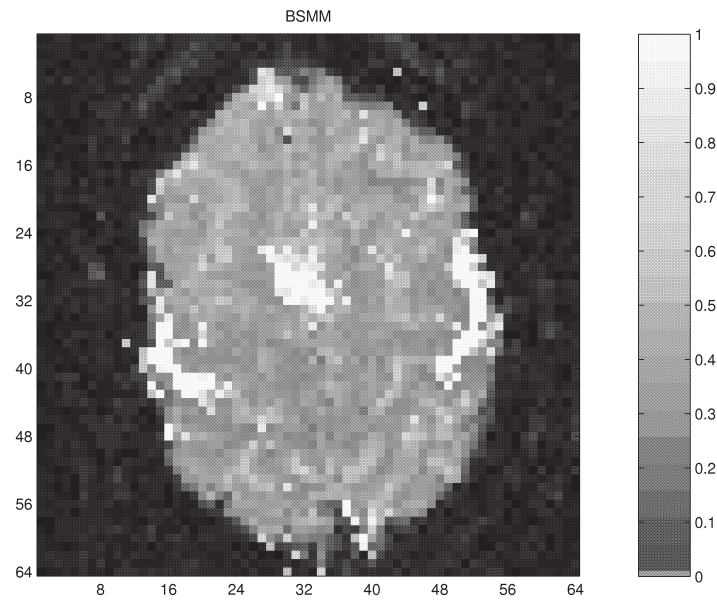


Fig. 11. Posterior probabilities from BSMM, with $N(-3, 1)$ prior

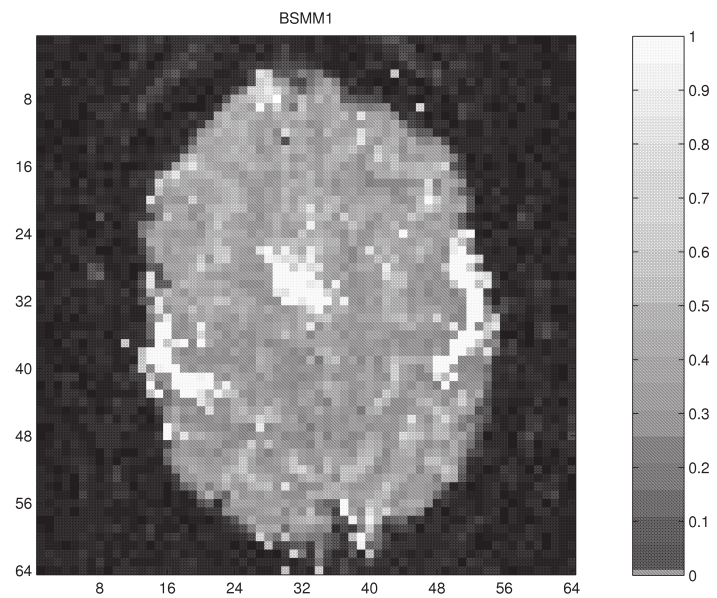


Fig. 12. Posterior probabilities from BSMM, with $N(-1.5, 1)$ prior

and $N(-1.5, 1)$ prior. Note that BSMM appears to capture more of the spatially distributed signal than the HJ model, without suffering from the overestimation of the activation region due to smoothing. Also, the BSMM in this case is not sensitive to the prior on β_0 since there is little difference between the posterior probabilities of activation with $N(-3, 1)$ prior on β_0 and a $N(-1.5, 1)$ prior.

All the simulations were programmed in C. The figures were produced with Matlab.

Discussion. In terms of bias, standard deviation and MSE, the BSMM tends to do better than the HJ spatial mixture model for a small- and modest-magnitude signal, but the performance is almost identical when the magnitude of the signal is high. The HJ model may be an option for large magnitude signals because it performs similarly and is computationally less intensive.

The methods were illustrated on a real data set from a bilateral finger-tapping fMRI experiment. The results from the real fMRI study confirm the conclusions from the simulation study.

REFERENCES

- [1] BANDETTINI P. A., A. JESMANOWICZ, E. C. WONG, J. S. HYDE. Processing strategies for time-course data sets in functional MRI of the human brain. *Magnetic Resonance in Medicine*, **30** (1993), 161–173.
- [2] BANERJEE S., B. P. CARLIN, A. E. GELFAND. Hierarchical Modeling and Analysis for Spatial Data. Chapman & Hall/CRC, 2004.
- [3] CARLIN B., T. LOUIS. Bayes and Empirical Bayes Methods for Data Analysis, Chapman & Hall/CRC, 2000.
- [4] CONSTABLE R. T., P. SKUDLARSKI, J. C. GORE. An ROC approach for evaluating functional brain MR imaging and postprocessing protocols. *Magnetic Resonance in Medicine*, **34** (1995), 57–64.
- [5] COX R. W., A. JESMANOWICZ, J. S. HYDE . Real Time functional Magnetic Resonance Imaging. *Magnetic Resonance in Medicine*, **33** (1995), 230–236.
- [6] EVERITT B., E. BULLMORE. Mixture Model mapping of brain activation in functional magnetic resonance images. *Human Brain Mapping*, **7** (1999), 1–14.

- [7] GELIAZKOVA M., B. LOGAN. Measuring the size of a region of activation in fMRI analysis. In: Proceedings of the American Statistical Association [CD-ROM], Minneapolis, MN, 2005, 213–218.
- [8] GELIAZKOVA M. Spatial Thresholding Procedures for fMRI Analysis. PhD thesis, 2007.
- [9] HARTVIG N., J. JENSEN. Spatial Mixture Modeling for fMRI data. *Human Brain Mapping*, **11** (2000), 233–248.
- [10] HIGDON D. Auxiliary variable methods for Markov Chain Monte Carlo with applications. *Journal of the American Statistical Association*, **93** (1998), 585–595.
- [11] ISING E. Beitrag zur Theorie des Ferromagnetismus. *Zeitschrift fur Physik*, **31** (1995), 253–258.
- [12] LOGAN B., M. GELIAZKOVA, D. ROWE. An Evaluation of spatial thresholding techniques in fMRI Analysis. *Human Brain Mapping*, **29** (2008), 1379–89.
- [13] LANGE N., S. C. STROTHER, J. R. ANDERSON, F. A. NIELSEN, A. P. HOLMES, T. KOLEND, R. SAVOY, L. K. HANSEN. Plurality and resemblance in fMRI data analysis. *Neuroimage*, **10** (1999), 282–303.
- [14] LUCIC A. S., M. N. WERNIC , S. C. STROTHER. An evaluation of methods for detecting brain activations from functional neuroimages. *Artificial Intelligence in Medicine*, **25** (2002), 69–88.
- [15] PAGANO M. , K. GAVREAU. Principles of Biostatistics. Duxbury Press, 1993.
- [16] SMITH M., B. PUTZ, D. AUER, L. FAHRMEIR. Assessing brain activity through Bayesian variable selection. *Neuroimage*, **20** (2003), 802–815.
- [17] SORENSEN J. A., X. WANG. ROC method for evaluation of fMRI techniques. *Magnetic Resonance in Medicine*, **36** (1996), 737–744.
- [18] SWENDSEN R., J. WANG. Non-universal critical dynamics in Monte Carlo simulations. *Physics Review Letters*, **58** (1987), 86–88.
- [19] WOOLRICH M. W., T. E. J. BEHRENS, C. F. BECKMANN, S. M. SMITH. Mixture Models with Adaptive Spatial Regularization for Segmentation with an application to fMRI data. *IEEE Transactions on Medical Imaging*, **24** (2005), 1–11.

- [20] XIONG J., J. GAO, J. L. LANCASTER, P. T. FOX. Assessment and optimization of functional MRI analyses. *Human Brain Mapping*, **4** (1996), 153–167.

Maya Geliazkova

*Stara planina st. bl. 2 vh. A ap. 11
8600 Yambol, Bulgaria
e-mail: maya.geliazkova@gmail.com*

Received June 15, 2010

Final Accepted September 19, 2010